

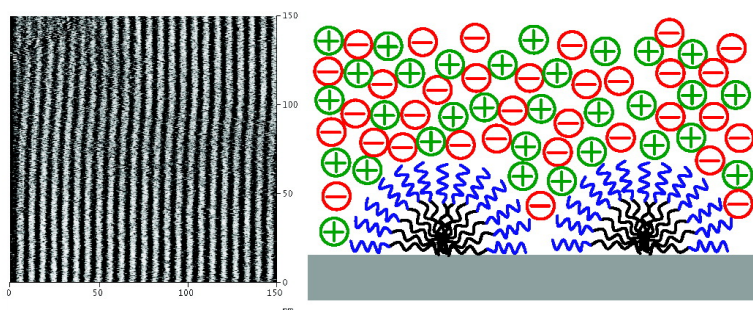
Communication

Self-Assembly of a Nonionic Surfactant at the Graphite/Ionic Liquid Interface

Rob Atkin, and Gregory G. Warr

J. Am. Chem. Soc., **2005**, 127 (34), 11940-11941 • DOI: 10.1021/ja053904z • Publication Date (Web): 06 August 2005

Downloaded from <http://pubs.acs.org> on March 25, 2009



More About This Article

Additional resources and features associated with this article are available within the HTML version:

- Supporting Information
- Links to the 18 articles that cite this article, as of the time of this article download
- Access to high resolution figures
- Links to articles and content related to this article
- Copyright permission to reproduce figures and/or text from this article

[View the Full Text HTML](#)

Self-Assembly of a Nonionic Surfactant at the Graphite/Ionic Liquid Interface

Rob Atkin* and Gregory G. Warr

School of Chemistry, The University of Sydney, NSW 2006, Australia

Received June 13, 2005; E-mail: r.atkin@chem.usyd.edu.au

Room temperature ionic liquids (ILs) are currently attracting considerable scientific interest as solvents for synthetic reactions, particularly those based on the imidazolium cation. Much of this interest stems from their environmentally friendly properties, most notably, low vapor pressure, and the ability to control some physical properties of the liquid by incorporation of appropriate functional groups.^{1–3} Recent studies have reported surfactant self-assembly in ILs, including micellization^{4,5} and microemulsion formation.⁶ A range of liquid crystalline phases, usually associated with aqueous systems, have been identified in ethylammonium nitrate (EAN),⁷ a hydrogen bonding IL.⁸ In this study, we demonstrate that EAN can support surfactant aggregate formation on graphite. This finding should allow hydrophobic particles, such as polymers or quantum dots, to be stabilized in hydrophilic ILs and may lead to new routes for the preparation of nanoscale structures.⁹

EAN was prepared by reacting equimolar amounts of ethylamine and nitric acid to produce an aqueous solution, as described by Evans et al.⁴ Excess water was removed by first purging the EAN solution with nitrogen, then heating at 110–120 °C for several hours under a nitrogen atmosphere. This leads to water contents undetectable by Karl Fischer titration and prevents the formation of nitrous oxide impurities that, if present, produce a yellow discoloration. 99% pure hexaethylene glycol monoheptadecyl ether ($C_{16}E_6$) was obtained from Fluka and used without further purification. The surfactant adsorbed layer morphology was investigated using a Digital Instruments NanoScope IIIa Multimode in contact mode. Cantilevers were standard Si_3N_4 with sharpened tips (Digital Instruments, CA). These were irradiated with ultraviolet light for 30 min prior to use. The same tip was used for all surfactant concentrations, permitting direct comparison of force data. The $C_{16}E_6$ -EAN solutions were held in a fluid cell sealed with a silicone O-ring. These were cleaned by sonication for 10 min in surfactant solution, rinsed copiously in ethanol and deionized water, and dried using filtered nitrogen. Graphite was prepared by using adhesive tape to cleave along the basal plane. Soft contact imaging¹⁰ was employed to study the surfactant layer. This method produces a force map of the adsorbed morphology without the tip physically contacting the sample. All images were obtained at room temperature, approximately 22 °C.

A deflection image of 30 wt % $C_{16}E_6$ adsorbed at the graphite-EAN interface is shown in Figure 1. Similar images were obtained for 10 and 20 wt % $C_{16}E_6$ in EAN. The striped appearance is strikingly similar to that reported for aqueous systems with similar surfactants.^{10–13} In water, the accepted adsorption mechanism involves two steps. Initially, a surfactant monolayer is adsorbed in a tail-to-tail arrangement along one of the three symmetry axes of graphite. Subsequent adsorption to form hemicylindrical aggregates is templated by this strongly bound underlayer.^{10–14} A comparable mechanism must be operating for the EAN system. Nonetheless, surface aggregation in EAN differs from that observed in water in several respects. First, the surface aggregation concentration is many orders of magnitude higher in EAN (~9 wt %) than in aqueous

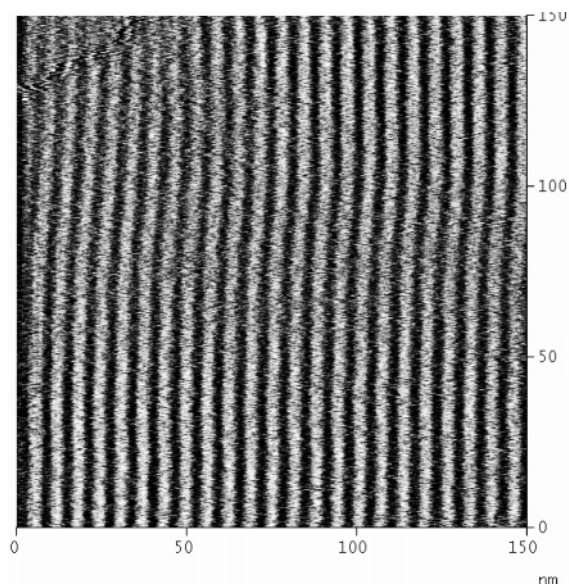


Figure 1. Deflection image of 30 wt % $C_{16}E_6$ adsorbed at the graphite-EAN interface. The hemimicelle aggregates have one short axis and one very long axis. The image presented has the scan angle perpendicular to the long axis, but identical structures were imaged at other scan angles. The height scale is 1 nm. The interaggregate periodicity was determined from the two-dimensional Fourier transform to be 6.3 nm, independent of scan angle.

solution ($\sim 8 \times 10^{-5}$ wt %),¹⁵ in line with the increased critical micelle concentration (cmc) for this surfactant in EAN.⁷ The nearest-neighbor separation of the hemimicelles is 6.3 nm in EAN, compared to 7.5 nm in water.¹³ This is because the surfactant headgroups are less extended in EAN than in water, due to a decreased level of hydrogen bonding. Recent neutron scattering experiments have detected a similar effect for nonionic micelles in bulk EAN solution.¹⁶ Finally, the critical chain length¹⁷ required for hemimicelle formation is greater in EAN than in water. In aqueous systems, surfactants with alkyl chain lengths shorter than C_{12} do not form cylindrical hemimicelles on graphite.^{12,15,17} This is postulated to be due to the weaker attraction between C_{10} (and shorter) chains and graphite, so that the initially adsorbed monolayer is not sufficiently well-ordered to template subsequent aggregation. We find a corresponding effect in EAN, with a weakly adsorbed layer but no lateral surface structure detectable for $C_{14}E_6$ at up to 50 wt %, but hemimicelles present for $C_{16}E_6$ above ~9 wt % solution. This is consistent with results for bulk surfactant aggregation in EAN, where it was found that surfactant tails 4 CH_2 units longer were required in EAN compared to water to produce similar liquid crystalline phases.⁷

Force curves for pure EAN and several concentrations of $C_{16}E_6$ in EAN are presented in Figure 2. For comparison, force curves for $C_{14}E_6$ in EAN and 4×10^{-3} wt % $C_{16}E_6$ in water ($50 \times$ cmc) are also presented. In pure EAN, a van der Waals attraction between the AFM tip and the graphite substrate from about 3 nm is evident,

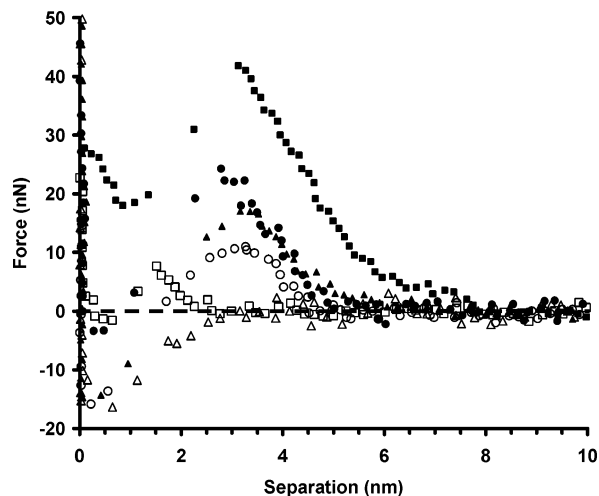


Figure 2. Force versus apparent separation for an AFM cantilever probe (Digital Instruments, Si_3N_4 , contact mode cantilever $k \sim 0.32 \text{ N m}^{-1}$) and a graphite substrate immersed in surfactant solutions. Closed symbols denote the presence of surface aggregates. Representative results are shown for 30 wt % C_{16}E_6 in EAN (\bullet), 15 wt % C_{16}E_6 in EAN (\blacktriangle), 8.5 wt % C_{16}E_6 in EAN (\circ), pure EAN (\triangle), 30 wt % C_{14}E_6 in EAN (\square), and 0.004 wt % C_{16}E_6 in H_2O (\blacksquare). Note the similar distance at which the AFM tip ruptures the surfactant film for aggregate forming systems in both water and EAN.

similar in form to that observed in aqueous systems. With added surfactant, a steep repulsion occurs beginning at a separation of $\sim 5 \text{ nm}$, consistent with the length of a fully extended C_{16}E_6 molecule. This repulsion is due to steric interactions between adsorbed surfactant and the bare AFM tip (see below). In comparison, the onset of the repulsive interaction in the aqueous system begins at 8 nm . This difference is most likely due to surfactant loosely bound to the AFM tip, although some authors have suggested a phase transition.¹² For concentrations where adsorbed aggregates were present, the AFM tip ruptures the surfactant film at a (“push-through”) separation of 3 nm . This can be seen in Figure 2 both for 15 and 30 wt % C_{16}E_6 in EAN and 4×10^{-3} wt % C_{16}E_6 in water. Similar results were found for 10 and 20 wt % C_{16}E_6 in EAN. This shows that the surfactant layer can be compressed to the same extent in EAN as water before the film is ruptured. However, the force required to reach this minimum distance is less in EAN than in water. This is due to the strength of solvophobic interaction between adsorbed surfactants, and between surfactants and the surface, being weaker in EAN than in water. This is also consistent with force curves acquired in pure EAN before and after 30 wt % C_{16}E_6 in EAN was contacted with substrate for a number of hours, which were essentially identical, suggesting that the underlayer can readily be desorbed from the graphite surface. This is in stark contrast to the situation in aqueous systems, where the layer in direct contact with the substrate is irreversibly adsorbed,^{14,15,17,18} and implies that the heat of adsorption of the lower monolayer must be considerably less in the EAN system.

Force curves for two systems where surface aggregates could not be imaged are also shown in Figure 2. For 8.5 wt % C_{16}E_6 in EAN, the push-through separation is about 1 nm less than that for the aggregate-forming systems, and the force required to rupture the adsorbed layer is also reduced. While surfactant is adsorbed at the interface, aggregate formation is incomplete at this concentration. The result for 30 wt % C_{14}E_6 is similar, but the push-through separation and force are lower still, suggesting even less adsorption.

Results similar in form were obtained for concentrations up to 50 wt % C_{14}E_6 , above which it precipitates at room temperature.

No evidence for adsorption of C_{16}E_6 onto hydrophilic silica from EAN could be detected from either force curves or imaging using the AFM at concentrations up to 30 wt %. Adsorption onto silica from aqueous solution is due to hydrogen bonding between the surfactant headgroup and surface silanol groups.¹⁹ In EAN, however, the cationic ethylammonium moiety evidently has a much greater affinity for surface sites than the surfactant, even at high surfactant concentrations.

Adsorption and surface aggregation in EAN has been shown to occur when there is a strong hydrophobic attraction between the surfactant tail and the surface. Increased surfactant concentrations and longer surfactant tail groups are required to produce surface aggregates in comparison to water. These observations may expand the usefulness of ILs by allowing the suspension of sterically stabilized hydrophobic particles or by providing a new reaction media for the preparation of nanoscale particles templated by the graphite substrate.

Acknowledgment. This work was supported by the Australian Research Council.

References

- (1) Forsyth, S. A.; Pringle, J. M.; MacFarlane, D. R. *Aust. J. Chem.* **2004**, *57*, 113–119.
- (2) Rodgers, R. D.; Seddon, K. R. *Science* **2003**, *302*, 792–293.
- (3) Seddon, K. R.; Stark, A.; Torres, M.-J. *Pure Appl. Chem.* **2000**, *72*, 2275–2287.
- (4) Evans, D. F.; Yamauchi, A.; Roman, R.; Casassa, E. Z. *J. Colloid Interface Sci.* **1982**, *88*, 89–96.
- (5) (a) Evans, D. F.; Yamauchi, A.; Wei, G. J.; Bloomfield, V. A. *J. Phys. Chem.* **1983**, *87*, 3537–3541. (b) Bowlas, C. J.; Bruce, D. W.; Seddon, K. R. *Chem. Commun.* **1996**, 1625–1626. (c) Gordon, C. M.; Holbrey, J. D.; Kennedy, A. R.; Seddon, K. R. *J. Mater. Chem.* **1998**, *8*, 2627–2636. (d) Firestone, M. A.; Dzielawa, J. A.; Zapol, P.; Curtiss, L. A.; Seifert, S.; Dietz, M. L. *Langmuir* **2002**, *18*, 7258–7260. (e) Yoshio, M.; Mukai, T.; Kanie, K.; Yoshizawa, M.; Ohno, H.; Kato, T. *Adv. Mater.* **2002**, *14*, 351–354. (f) Anderson, J. L.; Pino, V.; Hagberg, E. C.; Sheares, V. V.; Armstrong, D. W. *Chem. Commun.* **2003**, 2444–2445. (g) Yoshio, M.; Mukai, T.; Kanie, K.; Yoshizawa, M.; Ohno, H.; Kato, T. *Chem. Lett.* **2002**, 320–321. (h) Fletcher, K. A.; Pandey, S. *Langmuir* **2004**, *20*, 33–36.
- (6) (a) Eastoe, J.; Gold, S.; Rodgers, S. E.; Paul, A.; Welton, T.; Heenan, R. K.; Grillo, I. *J. Am. Chem. Soc.* **2005**, *127*, 7302–7303. (b) Gao, H. X.; Li, J. C.; Han, B. X.; Chen, W. N.; Zhang, J. L.; Zhang, R.; Yan, D. D. *Phys. Chem. Chem. Phys.* **2004**, *6*, 2914–2916.
- (7) Araos, M. U.; Warr, G. G. *J. Phys. Chem. B* **2005**, *109*, 14275–14277.
- (8) Beesley, A. H.; Evans, D. F.; Laughlin, R. G.; *J. Phys. Chem.* **1988**, *92*, 791–793.
- (9) Carswell, A. D. W.; O’Rear, E. A.; Grady, B. P. *J. Am. Chem. Soc.* **2003**, *125*, 14793–14800.
- (10) Patrick, H. N.; Warr, G. G.; Manne, S.; Aksay, I. A. *Langmuir* **1997**, *13*, 4349–4356.
- (11) (a) Manne, S.; Cleveland, J. P.; Gaub, H. E.; Stucky, G. D.; Hansma, P. K. *Langmuir* **1994**, *10*, 4409–4413. (b) Manne, S.; Gaub, H. E. *Science* **1995**, *270*, 1480–1482. (c) Wanless, E. J.; Ducker, W. A. *J. Phys. Chem.* **1996**, *100*, 3207–3214. (d) Ducker, W. A.; Grant, L. M. *J. Phys. Chem.* **1996**, *100*, 11507–11511.
- (12) Grant, L. M.; Tiberg, F.; Ducker, W. A. *J. Phys. Chem. B* **1998**, *102*, 4288–4292.
- (13) Blom, A. PhD Thesis, The University of Sydney, Australia, 2005.
- (14) Kiraly, Z.; Findenegg, G. H. *Langmuir* **2005**, *21*, 5047–5054.
- (15) Surface aggregation begins at concentrations slightly less than the cmc for similar systems. See: Findenegg, G. H.; Pasucha, B.; Strunk, H. *Colloids and Surfaces* **1989**, *37*, 223–233.
- (16) Araos, M. U.; Warr, G. G. Unpublished results.
- (17) Kiraly, Z.; Findenegg, G. H.; Mastalir, A. *J. Phys. Chem. B* **2003**, *107*, 12492–12496.
- (18) (a) Kiraly, Z.; Findenegg, G. H.; Klumpp, E.; Schlimper, H.; Dekany, I. *Langmuir* **2001**, *17*, 2420–2425. (b) Kiraly, Z.; Findenegg, G. H. *J. Phys. Chem. B* **1998**, *102*, 1203–1211. (c) Kiraly, Z.; Findenegg, G. H. *Langmuir* **2000**, *16*, 8842–8849.
- (19) Atkin, R.; Craig, V. S. J.; Wanless E. J.; Biggs, S. *Adv. Colloid Interface Sci.* **2003**, *103*, 219.

JA053904Z